Amplitude and Frequency Modulation Effects to Telemetry Link Reception

N. C. Ham
R. F. Systems Development Section

A spin-stabilized spacecraft can produce an amplitude and phase variation to the normally phase-modulated downlink carrier signal due to its antenna characteristics. The manifestation of these variations is equivalent to an amplitude and frequency modulation to the carrier signal, and the effects to the telemetry link must be considered. The Helios spacecraft and mission is a typical case, and means for simulating a certain portion of the flight profile, which will create such conditions, was utilized to test and evaluate the effect upon the DSIF Telemetry System. Initial test results indicated that the Telemetry System was more sensitive to the phase variation than to amplitude variations in increasing the detected symbol error rate for a given telecommunication link situation.

I. Introduction

Spin-stabilized-type spacecraft can alter the telecommunication link between the spacecraft and ground systems, particularly if the spacecraft RF antenna subsystem's physical placement is not coincident to the spacecraft spin axis and its radiation pattern is non-symmetrical containing lobes and deep nulls.

Typical is the case of the Helios spacecraft in its construction (Ref. 1) and mission flight maneuver phases. The spacecraft omni-directional antenna, which is comprised of simultaneously driven top dipole and bottom horn antenna elements, as shown in Fig. 1, produces a combined pattern envelope that is non-symmetrical on each side of the spin axis and for a radial polar revolution within the axis plane. The non-symmetry of each side of the axis is due to the horn antenna, which is displaced 6λ (wavelength at the transmitted frequency) from the spin axis. The polar asymmetry results from the linearly polarized, top dipole antenna and circularly polarized bottom horn antenna, where the top null is the top antenna "end-

fire" characteristic and lower portion nulls result from the interferometric effects of the combined top and bottom antennas.

During a spacecraft attitude maneuver (Step I: when the spacecraft aligns its axis normal to the Sun) early in the mission, the signal could possibly traverse through the lower antenna interference zone. The effect to the telecommunication link can be seen to vary the signal amplitude which is further compounded by the spacecraft rotation producing a periodic signal phase variation. A similar effect will occur during a later maneuver phase (Step II) when the spacecraft is commanded to align its spin axis perpendicular to the ecliptic plane.

The manifestation of these conditions is a phase variation expressed by $A_\lambda \sin 2\pi f_s t$ superimposed upon the normal phase-modulated, S-band, downlink signal, and an amplitude variation affecting this same signal to modify the carrier ($E_c \cos \omega_c t$) expressed as

$$e(t) = E_c (1 + A_m \cos 2\pi f_m t) \cos \omega_c t$$

where A_λ is related to the offset antenna distance of the horn antenna, f_s is related to the spacecraft rotation rate, A_m is related to the null depth in the antenna interference zone, and f_m is related to the omni-antenna pattern for one spacecraft revolution multiplied by the spacecraft rotation rate and "look angle."

Consider first the rotating spacecraft, with its offset antenna, traveling in a radial direction away from Earth with a radial velocity v. If the "look angle" is taken as being normal to the spin axis (a possible condition during Step II), as shown in Fig. 2, then the full value of the 6λ offset can be considered as the largest magnitude value for the rotating vector spinning within the plane of the radial velocity direction (see Fig. 3). The projected lateral component due to this rotating vector, parallel to the direction of radial velocity, is then $6\lambda \cos \Phi$, where Φ is the included vector angle. The spacecraft is revolving at an angular velocity ω of one revolution per second or, with an angular rate of change $d\Phi/dt = \omega = 2\pi f_s t = 2\pi t$; thus, the lateral component becomes $6\lambda \cos (d\Phi/dt)$ or $6\lambda \cos 2\pi t$ expressed as a function of time.

The radial velocity v imparts a Doppler frequency to the RF signal by the relation

$$F_{\text{Doppler}} = F_T \frac{c + v}{c - v}$$

where F_T is the frequency of the transmitted signal and c is the speed of light.

The displacement 6λ is also related to the transmitted frequency by $\lambda = c/F_T$. Since there are 2π radians per cycle of revolution, the above lateral component expression becomes $12\pi \cos 2\pi t$ and for one cycle of revolution $\Delta F_{\text{Doppler}} = 12\pi \cos 2\pi t$. The instantaneous doppler is the sum of the rotating component, with a magnitude of ± 37 Hz varying at a one-cycle rate, and the doppler due to the radial velocity v. This is shown in Fig. 4.

The rate of change of the component due to the spinning spacecraft can be obtained by the derivative of the above equation:

$$\frac{dF_D}{dt} = \frac{d}{dt} 12\pi \cos 2\pi t = -24\pi^2 \sin 2\pi t$$

or $\dot{F}_D = 240$ Hz per second. Thus, the phase variation of the ground received frequency results in a peak frequency deviation of ± 37 Hz about the radial velocity Doppler frequency, occurring periodically every second, with a 240-Hz per second rate change due to the spinning spacecraft.

The gain variation of the antenna produces an amplitude-modulated carrier signal with an envelope that is cusp-serrated, as shown in Fig. 5 modeled from a typical spacecraft antenna pattern for one revolution and specific "look angle" of Fig. 6. This can be approximated as a time varying function where $f_m = 20$ Hz and $A_m = 10$ dB when considering only the higher frequency components of the Fig. 6 rotation-time function characteristics.

It becomes a concern for the mission operation as to the degree of additional degradation to the normal telemetry telecommunication link that may be contributed from this condition. The Deep Space Station Telemetry System is comprised of the receiver subsystem which phase and amplitude tracks the modulated carrier using electronic servo loops, the Subcarrier Demodulator Assembly (SDA) for creating a local estimate of the bi-phase modulated subcarrier for data demodulation of the sideband energy, the Symbol Synchronizer Assembly (SSA) for data synchronization, and a Data Decoder Assembly (DDA) for sequentially decoding the convolutional-encoded telemetry when the coded mode is utilized.

Based on the postulated conditions and modeled signal variations, a quick analysis of the Telemetry System performance is presented in the following discussion.

II. Receiver Automatic Gain Control Loop Response

The Automatic Gain Control (AGC) closed loop $H(j\omega)$ amplitude response is shown in Fig. 7 for the widest bandwidth (BW) value with a resulting −3-dB amplitude value corresponding to 6 Hz (Ref. 1). With the postulated 20-Hz periodic amplitude-variation input applied, the AGC response curve indicates a −10-dB value, and consequently the gain control loop cannot track or follow this rate but instead responds only to the average of the signal variations. This average value is approximately 1 dB higher in value than the non-amplitude-modulated condition and due to the variations produces a resultant carrier and sideband fluctuation at the IF amplifier output as shown in Fig. 8. The variation is a periodic +3-dB increase and −7-dB decrease from the average or control level value.

The only AGC loop anomaly that may result from this instantaneous −7-dB carrier decrease is that the receiver loop "in-lock" detector, which reacts to the carrier amplitude, may momentarily disengage if the decrease in signal and duration approaches the "in-lock" circuit time constant. An instantaneous disengagement can produce an erroneous "flag" to the telemetry data stream block.

III. RF Loop Response

The receiver carrier phase-locked loop employs a bandpass limiter whose input-signal level "set point" is related to the absolute value of the carrier as established by the AGC loop. The "set point" is well beyond the limiter "knee" such that a −8-dB (−7 dB plus −1 dB due to AGC control level change) instantaneous decrease, at strong signal conditions, will still develop a constant limiter output value (see Fig. 9). Since the RF loop bandwidth determination involves an amplitude parameter which is still maintained constant by the limiter, the loop will remain "in-lock" and develop a normal operating bandwidth.

The above condition applies regardless of the RF loop bandwidth value; however, the input Doppler and Doppler rate will produce phase errors within the loop and to the local estimate of the carrier phase. For example, if the bandwidth of 152 Hz is used, an additional phase error due to the rotating 6λ offset horn of no more than 3-deg peak will result (Ref. 1).

IV. Subcarrier Demodulator Response

The SDA, which utilizes a phase-locked loop, should be operated in the medium loop bandwidth value for reducing phase tracking errors. This loop has a "soft limiter" circuit, as contrasted to the carrier loop "hard limiter," and although the SDA limiter output varies proportionally to the input value (at strong signal levels), the loop will remain "in-lock" and maintain a constant loop BW since the loop low-pass filter averages the variations (Ref. 2). The Doppler rate-to-SDA loop BW ratio at the subcarrier frequency is considerably lower than for the carrier case and since the SDA loop is also a second-order type, it produces only a small resultant phase error when tracking the input-signal phase variations.

The SDA data-demodulation channel achieves the demodulation by a phase-coherent amplitude detector circuit; hence, the demodulated data have the same signal amplitude variations. The momentary data amplitude increase, during high signal-to-noise ratio (SNR) conditions, will not encounter signal suppression since the dynamic range of the circuits possesses ample amplitude linearity range. See Fig. 10, which also illustrates the time relationship of the signal duration (128 symbols per second (sps)) to the amplitude variation envelope and null depth. The SDA is also equipped with an "in-lock" detector, similar to the carrier AGC circuit, but it reacts instead to the data amplitude; therefore, its response to the varying sideband amplitude follows a similar consideration.

V. Symbol Synchronizer Response

The SSA is similarly comprised of a phase-locked, symbol-tracking loop for symbol synchronization and a symbol-detection channel (Ref. 3).

The symbol-tracking loop will remain "in-lock" to the input variation, where again the Doppler rate is low at this symbol frequency. Since the loop integration occurs symmetrically about the symbol transition point, the loop is unperturbed by the amplitude variations or noise at a high input SNR.

The symbol detection channel will operate with only slight degradation because its data-type selector uses the

sign bit of the symbol value (from the channel integrate-and-dump circuit) to determine whether the symbol is a logical 1 or a logical 0 and the amplitude linearity is adequate to handle the amplitude increases. Also, should it be necessary to increase the overall level of the symbols (an SDA operational adjustment) to insure that the minimum value of the symbol is always above the threshold value, this can be easily accommodated to enhance its performance capability.

VI. Data Decoder Response

In the coded-mode case the symbol duration time must be considered, for here the symbol rate is 256 symbols per second and the SSA, which outputs the detected symbols to the DDA for decoding the convolutional encoded data, now has a shorter symbol duration-to-envelope variation time ratio (see Fig. 10). As far as the DDA performance is concerned, only relatively slight degradation is expected since the symbol value output from the SSA is a binary number related to the polarity and amplitude of the voltage in the SSA integrator (at the end of the symbol time) and the expected amplitude will be above the DDA threshold designed value. If an occasional symbol error due to amplitude variations randomly occurs (at a frequency no greater than one in ten), then no degradation is expected – especially at high SNR.

VII. Simulated System Test

Figure 11 is a block diagram of the test configuration that was used at the JPL Compatibility Test Area (CTA 21) to simulate the above conditions and evaluate the Telemetry System performance. The signal generator (shown driving the exciter VCO) simulates the phase variation, where the amplitude of the generator signal relates to the 6λ offset or frequency deviation, and the generator frequency to the spacecraft rotation rate. The function generator, and circuitry following the translator output, simulates the amplitude variation due to the antenna interference zone, where the generator frequency and signal level set these parameters. The function circuitry is a simple diode-bridge rectifier which accepts the sine-wave signal from the generator and develops a full-wave rectified output waveform simulating the amplitude cusp-serrated envelope. The power amplifier amplifies this signal and modulates the PIN (P-intrinsic-N) modulator. The PIN modulator contains a number of PIN diodes mounted as shunt elements across a transmission line. Because of their appreciable storage time, they do not rectify the S-band signal; however, when a dc forward bias is applied, the diode conducts, reducing their resistance with low reactance, and shunts the transmission line. This functions as an absorption modulator, with virtually no incidental frequency modulation, and a simulated amplitude-variation signal is thereby achieved.

The variable attenuator is used to establish the average signal level which is used as the independent variable parameter for the test conditions. The Simulation Conversion Assembly (SCA) generates a 128-symbol per second PN sequence pattern (uncoded mode test configuration) for modulating the exciter simulating the spacecraft telemetry stream, and simultaneously a reference stream to the Telemetry and Command Processor (TCP) for a symbol-by-symbol comparison with the detected data to compute symbol-error-rate (SER) statistics. A typical test run procedure was to establish a particular signal-level margin M above the RF loop threshold value and observe the SER (computed for a sampling size of 10^4 symbols) with various combinations of simulated amplitude and frequency modulation applied.

Although a high SNR setting (when no AM and FM is applied) results in a low probability of SER, the value of 1×10^{-4} was set as a minimum value for evaluation comparison when modulation is applied. Thus, any degradation that may occur due to the simulation would produce nearly instantaneous symbol errors occurring at a periodic rate of the simulation FM and AM frequencies. The criterion for system failure is orders-of-magnitude SER increase during simulation modulation. The ratio of the 10^4 symbol time duration to the AM/FM frequencies duration (50 seconds to 50 milliseconds and 1 second) was considered adequate for gathering error statistics. The rationale was to reduce extremely long test runs at this low symbol rate for each adjusted signal level setting.

The same procedure was followed for the coded-mode test configuration except that frame erasures were used as the parameter for comparative purposes.

The monitor equipment was used to calibrate and monitor the various points throughout the Telemetry System to insure that the results were correct and to validate the simulation. For example, a base band signal of 1 kHz was used to calibrate the modulation depth of the AM simulation by observing the phase-demodulated envelope pattern at the receiver phase detector output (normally used for pre-detection recording) after bypassing the detector limiter circuit.

VIII. Test Results

The following conditions were used for the system test:

RF loop BW	152 and 48 Hz
AGC loop BW	Wide
SDA loop BW	Medium
SSA loop BW	Medium
SDA mod index attenuator	Normal setting
Modulation index	68.2° (−8.6-dB carrier suppression)
Subcarrier frequency	32,768 Hz
Symbol rate (uncoded)	128 bps
Symbol rate (coded)	256 sps
Bit rate (coded)	128 bps
AM (period)	20 Hz
FM (deviation)	±37 Hz
FM (period)	1 Hz
Data Format:	
Uncoded	2047-bit PN sequence
Convolutional coded	192 bits/frame

Tables 1 through 7 are tabulations of the results obtained from the various test combinations.

Table 1 is the resulting SER for 128-bit per second (bps) uncoded data and an AM null depth of 10 dB applied with an RF loop BW of 152 Hz and the remaining test conditions as stated above. This table indicates that the FM phase variation produced only slight degradation when the signal level is 10 dB or greater above the RF loop threshold value, as expected, since the additional loop phase error contributions were analyzed to be approximately 3 deg at a 10-dB margin; similarly, the degradation is slight with AM applied in addition to FM.

Table 2 is the SER for 128-bps uncoded similar to conditions of Table 1 except that an RF BW of 48 Hz was used. Here it is seen that FM has quite an effect upon the degradation since an evaluation of the RF loop indicates that the phase error is approximately 20 deg (at a signal margin of 10 dB), with the applied 240-Hz per second Doppler rate, as compared to only 3 deg for the 152-Hz BW (Ref. 1).

Figure 12 is a plot of the SER versus the signal margin M from this same test run.

Table 3 is a direct comparison of the RF loop BW of 152 Hz versus 48 Hz showing the doppler rate effect to the lower BW value for the combined AM/FM applied case.

Table 4 conditions are similar to Table 1 except that the AM depth was increased from 10 dB to 13.6 dB and shows that this null depth contributes very little additional degradation compared to the FM-only condition.

Table 5 compares the 10-dB AM depth to the 13.6-dB depth for the RF BW value of 152 Hz for both AM/FM applied and shows surprising identical results indicating that the Telemetry System is not sensitive to AM over this range of AM depth when the margin is 10 dB or greater.

Table 6 tabulates the results of the convolutional-coded mode similar to the uncoded mode test conditions of Table 1. The sample run time was 10 minutes for each of the signal margin levels.

Table 7 combines the results shown in Table 1 and Table 6, uncoded versus coded mode simply to show that the 10-dB RF loop margin value appears to a "criteria point" below which degradation begins to become apparent.

IX. Conclusions

As stated previously, a 10-dB margin above RF loop design threshold value (for this particular modulation index and BW settings) was the signal level where detection error changes became noticeable. A signal margin of 15 dB or greater would insure that the postulated signal variation would produce negligible degradation to the DSS Telemetry System performance.

The Telemetry System was more sensitive to the phase variations than to the amplitude variations as shown by Tables 3 and 5. This is a particularly important factor since these results are applicable to the "uplink" signal transmission to the spacecraft if similar type demodulation/detection systems are employed. Briefly stated, the most severe Doppler and Doppler rate values occur at the carrier frequency, and RF loop circuits that must track this signal could produce phase errors which contribute largest to the overall degradation. Since the amplitude variations below the AGC average value were of short duration, the "in-lock" circuits did not fluctuate or develop erroneous "flags" as first assumed.

The performance to either the coded or uncoded mode for these specific formats produced comparable results.

The foregoing analysis and Telemetry System test, based on the modeled input condition, were not intended to be rigorous but was structured to observe the first-order effects; hence, a more detailed analysis would be required for a complete performance evaluation covering more facets of possible conditions. Suffice it to say, the test method and results appear valid and support the quick analysis; furthermore, information presently available pertaining to performance characteristics of the individual subsystems can be used as an intuitive guide for evaluating the expected systems performance — or, at least, to formulate a system test method.

It should be clarified here that these results were the effects due to the rotating offset spacecraft antenna and a typical omni-antenna pattern and should be considered as additional factors that would contribute to any specific condition. Thus, the Doppler effects resulting from trajectory dynamics must certainly be included for a complete performance evaluation.

References

1. *Deep Space Network/Helios Spacecraft Telecommunication Interface Definition*, Document 613-6, Dec. 1, 1972 (JPL internal document).
2. Brockman, M. H., "MMTS: Performance of Subcarrier Demodulator," in *The Deep Space Network*, Space Programs Summary 37-52, Vol. II, pp. 127–141. Jet Propulsion Laboratory, Pasadena, Calif., July 31, 1968.
3. Frey, W., Petrie, R., and Greenberg, R., "Multiple-Mission Telemetry System Project," in *The Deep Space Network*, Space Programs Summary 37-61, Vol. II, p. 125. Jet Propulsion Laboratory, Pasadena, Calif., Jan. 31, 1970.

Table 1. SER comparison of FM against AM/FM applied

Test mode	M = 27 dB	M = 17 dB	M = 12 dB	M = 10 dB
With FM	$<10^{-4}$	$<10^{-4}$	$<10^{-4}$	4.8×10^{-4}
With AM/FM	$<10^{-4}$	$<10^{-4}$	1.6×10^{-4}	4.5×10^{-4}
RF BW = 152 Hz, 10-dB AM depth, 128 bps uncoded				

Table 2. SER comparison of AM against AM/FM applied

Test mode	M = 15 dB	M = 12 dB	M = 10 dB	M = 5 dB
With AM	$<10^{-4}$	$<10^{-4}$		
With AM/FM	2.47×10^{-3}	4.5×10^{-2}	1.0×10^{-1}	2.2×10^{-1}
RF BW = 48 Hz, 10-dB AM depth, 128 bps uncoded				

Table 3. SER comparison of RF BW 152 Hz versus 48 Hz

Test mode	M = 16 dB	M = 15 dB	M = 12 dB	M = 10 dB
152 Hz AM/FM	$<10^{-4}$	$<10^{-4}$	1.6×10^{-4}	4.5×10^{-4}
48 Hz AM/FM	3.5×10^{-3}	2.47×10^{-3}	4.5×10^{-2}	1.0×10^{-1}
10-dB AM depth, 128 bps uncoded				

Table 4. SER FM versus AM/FM comparison with 13.6-dB AM

Test mode	M = 28 dB	M = 20 dB	M = 16 dB	M = 10 dB
With FM		$<10^{-4}$	$<10^{-4}$	3.3×10^{-4}
With AM/FM	$<10^{-4}$	$<10^{-4}$	$<10^{-4}$	4.1×10^{-4}
RF BW = 152 Hz, 13.6-dB AM depth, 128 bps uncoded				

Table 5. SER comparison of 10-dB versus 13.6-dB AM depth

Test mode	M = 28 dB	M = 20 dB	M = 16 dB	M = 10 db
10-dB AM depth	$<10^{-4}$	$<10^{-4}$	$<10^{-4}$	4.5×10^{-4}
13.6-dB AM depth	$<10^{-4}$	$<10^{-4}$	$<10^{-4}$	4.1×10^{-4}
RF loop = 152 Hz, AM/FM applied, 128 bps uncoded				

Table 6. Frame erasure comparison for coded mode

Test mode	M = 20 dB	M = 15 dB	M = 10 dB	M = 7 dB	M = 3 dB
No AM, FM	None	None	None	8 Erasures	>100 Erasures
With AM/FM	None	None	None	9 Erasures -	>100 Erasures
RF BW = 152 Hz, 10-dB AM depth, 128 bps coded					

Table 7. Comparison of uncoded versus coded with AM/FM

Test mode	M = 15 dB	M = 10 dB	M = 7 dB
Uncoded SER	$<10^{-4}$	4.5×10^{-4}	
Coded erasure	No erasures	No erasures	9 erasures
RF BW = 152 Hz, 10-dB AM depth			

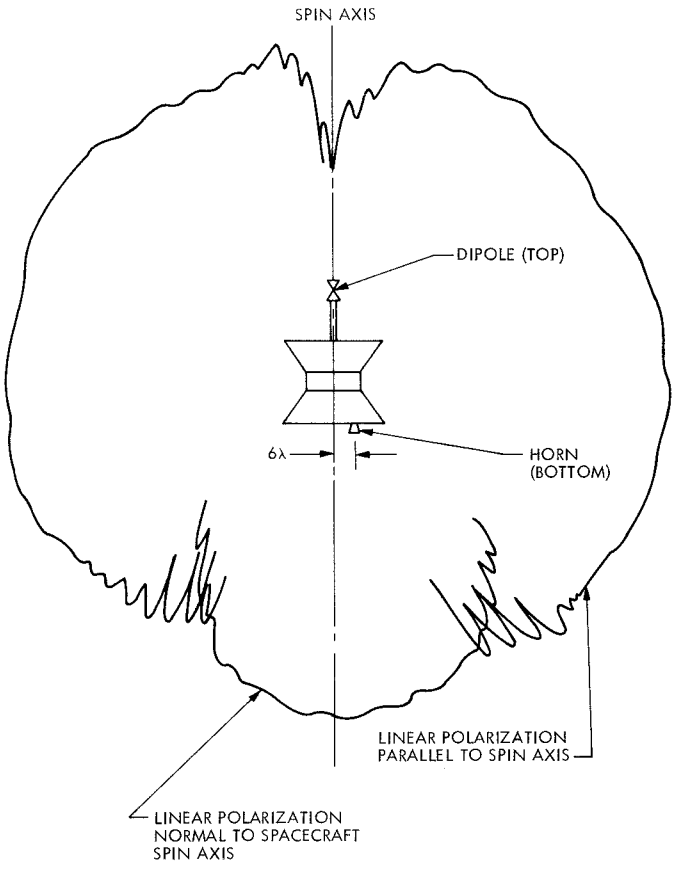

Fig. 1. Spacecraft omni-antenna pattern in plane through spin axis

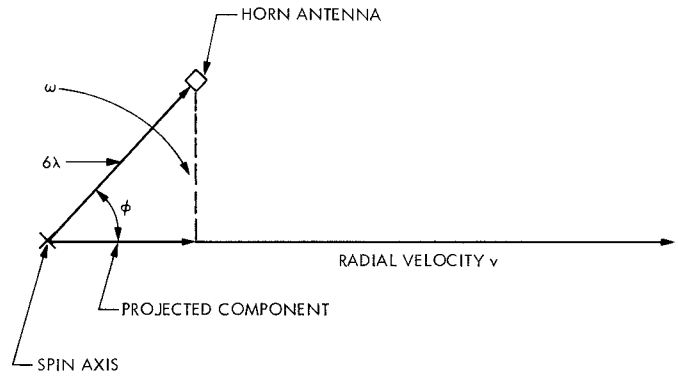

Fig. 3. Rotating spacecraft with off-axis RF antenna in plane normal to spin axis

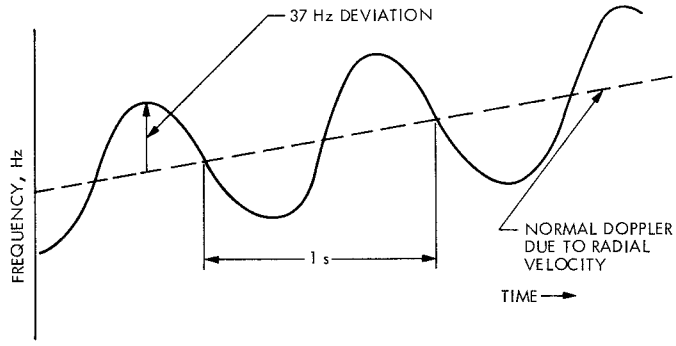

Fig. 4. Resultant instantaneous Doppler frequency due to rotating spacecraft traveling at a radial velocity

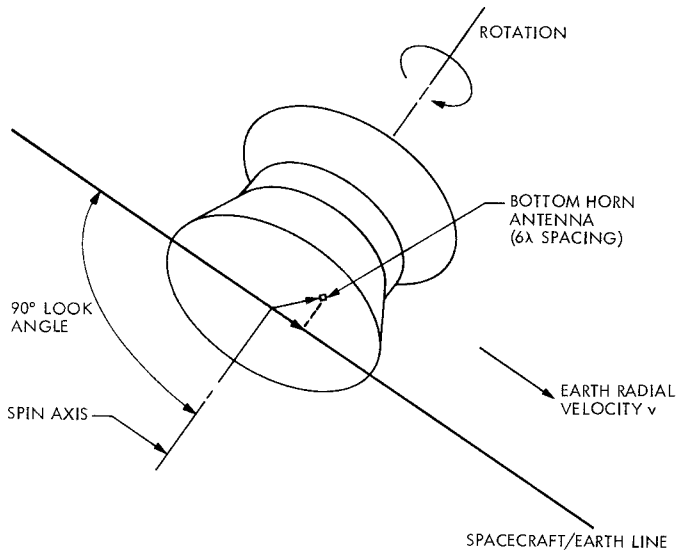

Fig. 2. Rotating spacecraft with off-axis RF antenna as seen from Earth

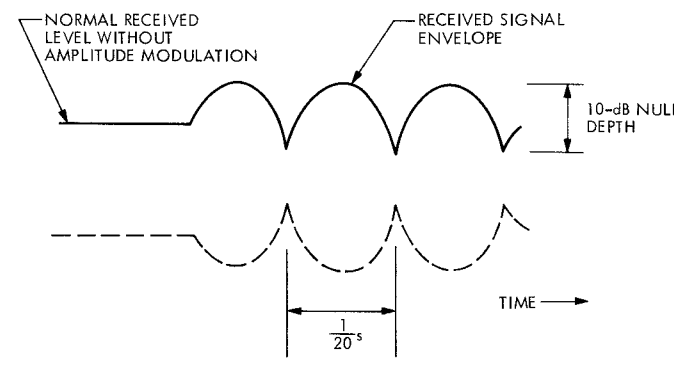

Fig. 5. Modeled amplitude-modulated signal due to low-gain antenna characteristic

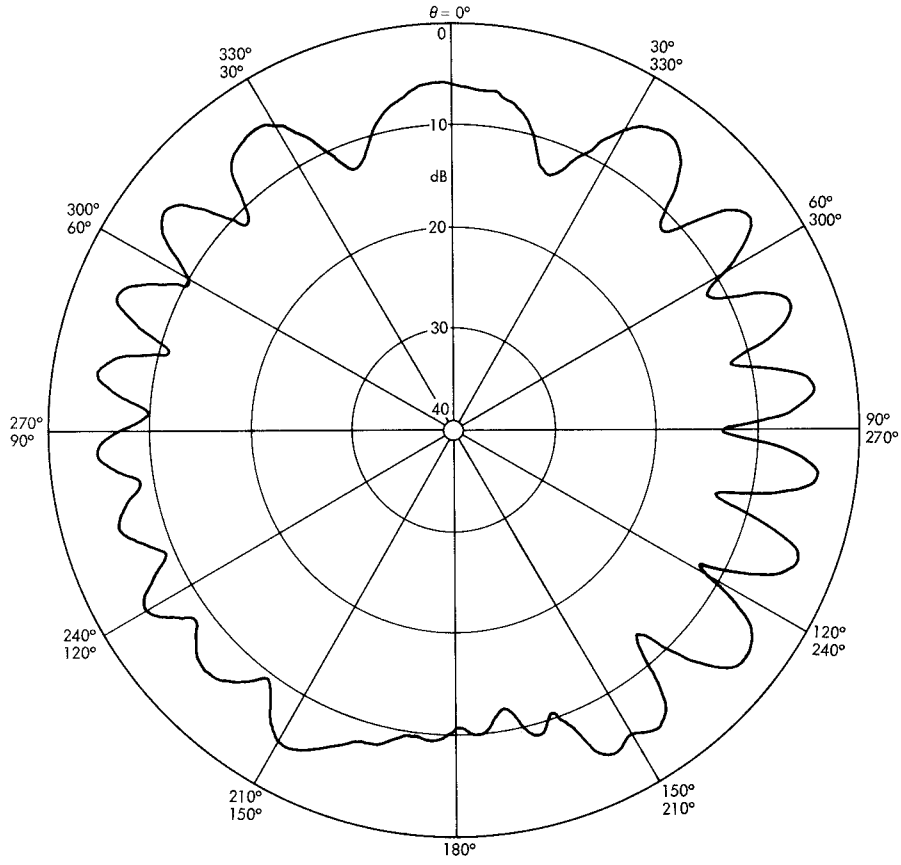

Fig. 6. Typical combined LGA pattern plotted through interference zone for one revolution

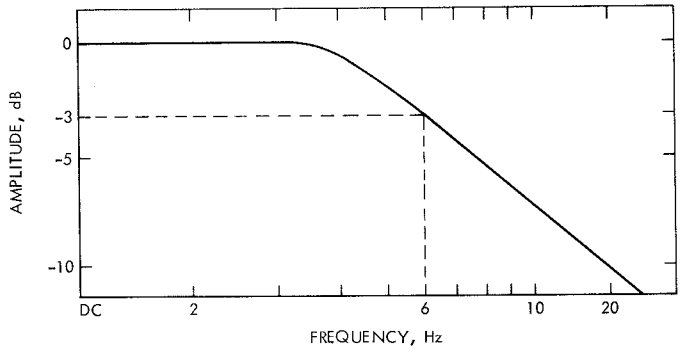

Fig. 7. Closed loop H(jω) AGC amplitude response

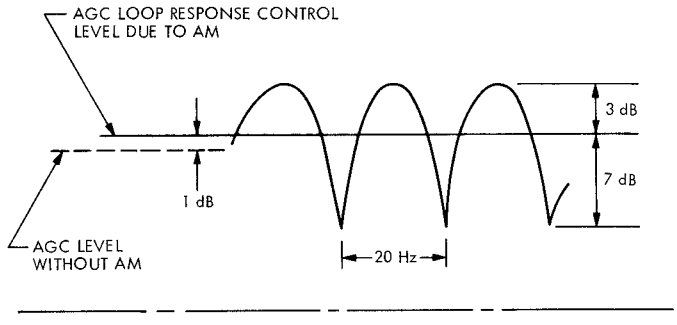

Fig. 8. Gain control level of AGC loop to modulated signal

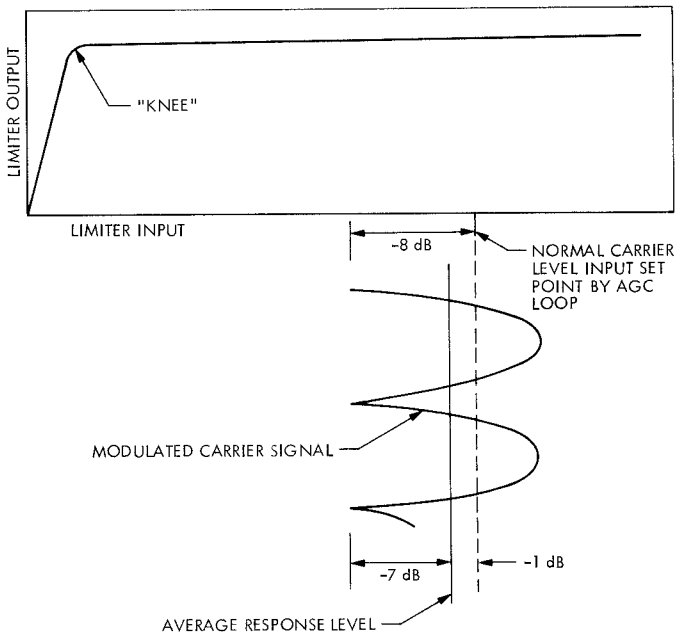

Fig. 9. RF loop limiter characteristic

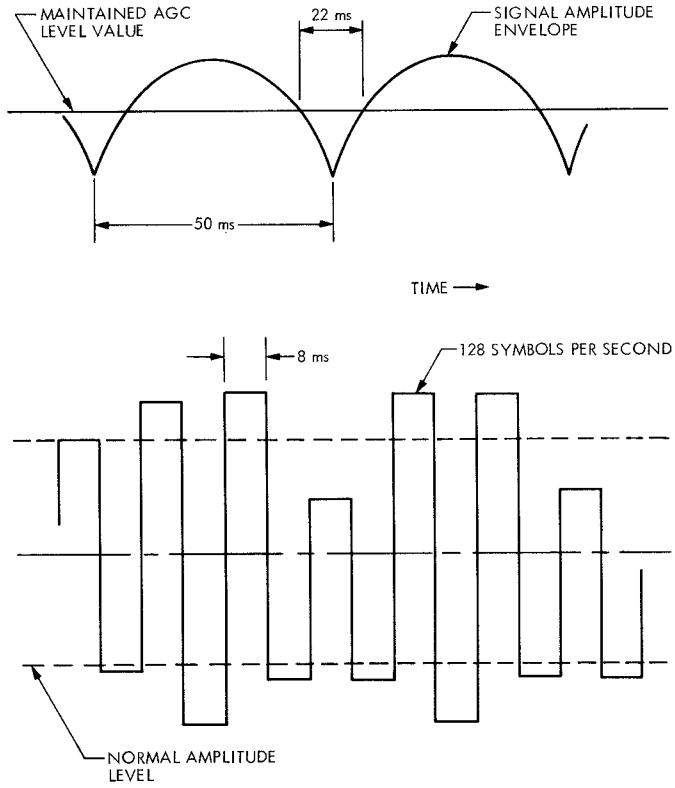

Fig. 10. Resultant SDA demodulated data amplitude and time relationship

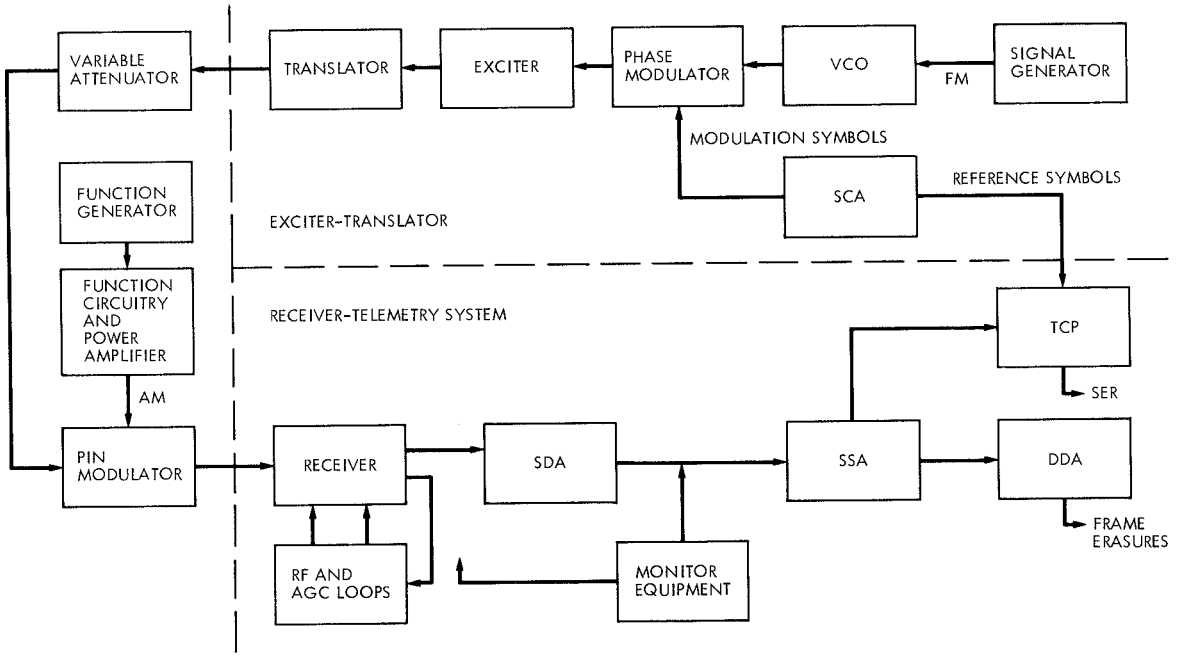

Fig. 11. Block diagram of simulation system test

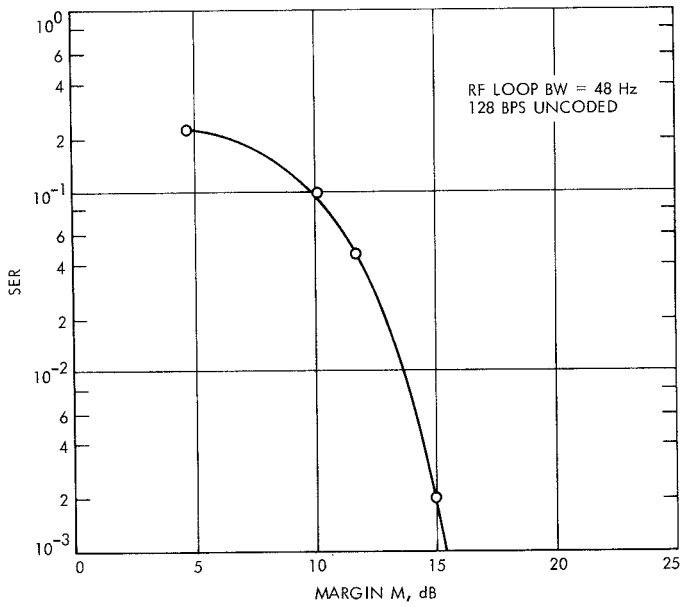

Fig. 12. SER versus M with AM/FM applied as obtained from Table 2 data